Journal of Oleo Science
Copyright ©2013 by Japan Oil Chemists' Society
J. Oleo Sci. **62**, *(12) 1029-1039 (2013)*

Two-Component Langmuir Monolayers and LB Films of DPPC with Partially Fluorinated Alcohol (*F*8*H*9OH)

Hiromichi Nakahara, Chikayo Hirano and Osamu Shibata*

Department of Biophysical Chemistry, Faculty of Pharmaceutical Sciences, Nagasaki International University; 2825-7 Huis Ten Bosch, Sasebo, Nagasaki 859-3298, Japan

Abstract: The interaction of (perfluorooctyl)nonanol (*F*8*H*9OH) with dipalmitoylphosphatidylcholine (DPPC) was systematically studied in two-component monolayers at air–water interface. The thermodynamic property and phase morphology of the monolayers were investigated by isotherm measurements and several microscopic methods such as Brewster angle microscopy, fluorescence microscopy, and atomic force microscopy (AFM). The AFM topographies for Langmuir-Blodgett films of *F*8*H*9OH exhibit the formation of monodispersed surface micelles. In the two-component system, the incorporation of *F*8*H*9OH induces condensation (or solidification) of DPPC monolayers. The excess Gibbs free energy and interaction parameter (or energy) of the two components were calculated from the isotherm data. Both the phase transition pressure for the coexistence of ordered and disordered phases and collapse pressure of monolayers vary with the mole fraction of *F*8*H*9OH, indicating binary miscibility between *F*8*H*9OH and DPPC within a monolayer state. The miscibility is also confirmed visually by *in situ* and *ex situ* microscopy at micro- and nanometer scales.

Key words: Langmuir monolayer, lung surfactant, DPPC, fluorinated amphiphile, surface pressure, surface potential

1 INTRODUCTION

Dipalmitoylphosphatidylcholine (DPPC) is a major lipid in pulmonary surfactants (PS) and not in biomembranes[1-3]. PS films line the air-alveolar fluid interface and show specific changes in fluidity and rigidity during respiration. We have focused our attention on the regulation of fluidity, phase behavior, and interfacial property of DPPC monolayers at the air-water interface by the incorporation of fluorinated compounds. Fluorinated amphiphiles are attractive because of their unique properties such as combined hydrophobicity and lipophobicity[4], high gas-dissolving capacity, chemical and biological inertness, low surface tension, and high fluidity[4, 5]. These fundamental properties and potential applications for the industrial and medical fields have been reviewed[6, 7]. So far, the interactions of fluorinated amphiphiles with DPPC have been elucidated utilizing perfluorocarboxylic acids[8, 9] and partially fluorinated amphiphiles[10-15]. The most studied fluorinated amphiphiles include a series of $CF_3(CF_2)_{n-1}(CH_2)_mCOOH$ or *FnHm*-COOH[16-19]. Although the physiochemical properties of fluorinated carboxylic acids have been well characterized, their interactions with other compounds have not been well investigated. The interactions of carboxylic acids results from the complex balance of dissociation and association in the carboxylic groups, which strongly depend on the experimental conditions such as pH. The combination of carboxyl groups and carboxylate anions in *FnHm*COOH molecules suppresses the potential interaction between the hydrophobic chains of the acid and guest molecules. Therefore, we have shifted our attention to $CF_3(CF_2)_{n-1}(CH_2)_mOH$ or *FnHm*OH molecules, which is not easily affected by pH. The fluidity of DPPC monolayers is perturbed by the addition of *F*8*Hm*OH molecules[11, 12], i.e., such perturbation is significantly related to the total chain length or fluorination degree in an *F*8*Hm*OH molecule. In fact, the incorporation of *F*8*H*5OH molecules cause a fluidization of the DPPC monolayers[12]. On the other hand, longer *F*8*H*11OH molecules show a solidifying effect on them[11]. Recently, an unusual relationship has been reported for the binary DPPC/*F*8*H*7OH monolayers[20]: the two components interact less at low surface pressures while a strong interaction was observed between them at high surface pres-

*Correspondence to: Osamu Shibata, Department of Biophysical Chemistry, Faculty of Pharmaceutical Sciences, Nagasaki International University, 2825-7 Huis Ten Bosch, Sasebo, Nagasaki 859-3298, Japan
E-mail: wosamu@niu.ac.jp
Accepted July 5, 2013 (received for review June 1, 2013)
Journal of Oleo Science ISSN 1345-8957 print / ISSN 1347-3352 online
http://www.jstage.jst.go.jp/browse/jos/ http://mc.manusriptcentral.com/jjocs

sures. Thus, the degree of fluorination in partially fluorinated chains may produce an unexpected interaction with lipids.

Herein, we extend the studies on the mutual interaction between fluorinated amphiphiles and DPPC. The interfacial behavior and lateral interaction for the binary DPPC/*F*8*H*9OH system were elucidated by a Langmuir monolayer. The surface pressure (π)–molecular area (A) and surface potential (ΔV)–A isotherms were measured (thermodynamic data). The phase behavior and monolayer morphology were visually observed by Brewster angle microscopy (BAM), fluorescence microscopy (FM), and atomic force microscopy (AFM). The miscibility between the two components was systematically investigated on macro/nanoscale. Furthermore, compared to the previous data for the binary DPPC/*F*8*Hm*OH systems[11, 12, 20], we describe a relationship between the fluorination degree in *F*8*Hm*OH and interaction with DPPC monolayers.

2 EXPERIMENTAL

2.1 Materials

(Perfluorooctyl)nonanol (*F*8*H*9OH) was synthesized via a previously reported procedure[21]. L-α-Dipalmitoylphosphatidylcholine (DPPC; purity >99%) and the fluorescent probe, 1-palmitoyl-2-[6-[(7-nitro-2-1,3-benzoxadiazol-4-yl)amino]hexanoyl]-*sn*-glycero-3-phosphocholine (NBD-PC), were obtained from Avanti Polar Lipids (Alabaster, AL). These lipids were used as received without further purification. n-Hexane (>98.5%) and ethanol (>99.5%) were obtained from Merck KGaA (Uvasol, Darmstadt, Germany) and nacalai tesque (Kyoto, Japan), respectively. The n-hexane/ethanol (9/1, v/v) mixture was used as the spreading solvent. Sodium chloride (nacalai tesque) was roasted at 1023 K for 24 h to remove all the surface active organic impurities. The subphase solution was prepared using thrice distilled water (surface tension = 72.0 mN m^{-1} at 298.2 K; electrical resistivity = 18 MΩ cm).

2.2 Methods

2.2.1 Surface pressure-area isotherms

The surface pressure (π) of monolayers was measured using an automated custom-made Wilhelmy balance. The surface pressure balance (Mettler Toledo, AG-245) had a resolution of 0.01 mN m^{-1}. The pressure-measuring system was equipped with filter paper (Whatman 541, periphery = 4 cm). The trough was made from Teflon-coated brass (area = 720 cm^2). Teflon barriers (both hydrophobic and lipophobic) were used in this study. The π–molecular area (A) isotherm was recorded at 298.2 ± 0.1 K. The stock solutions of DPPC (1.0 mM) and *F*8*H*9OH (1.0 mM) were prepared in n-hexane/ethanol (9/1, v/v). The spreading solvents were allowed to evaporate for 15 min prior to compression. The monolayer was compressed at a speed of ~0.10 nm^2 molecule^{-1} min^{-1}. The standard deviations (SD) for A and π were ~0.01 nm^2 and ~0.1 mN m^{-1}, respectively[12, 22, 23].

2.2.2 Surface potential-area isotherms

The surface potential (ΔV) and π were recorded simultaneously when the monolayer was compressed at the air-water interface. The process was monitored using an ionizing ^{241}Am electrode, which was placed at 1–2 mm above the interface, while a reference electrode was dipped in the subphase. The electrometer (Keithley 614) was used for the ΔV measurement. The SD for ΔV was 5 mV[24, 25].

2.2.3 Brewster angle microscopy (BAM)

The monolayer was directly visualized at the air-water interface by a Brewster angle microscope (KSV Optrel BAM 300, KSV Instruments Ltd., Finland) coupled to a commercially available film balance system (KSV Minitrough, KSV Instruments Ltd.). The use of a 20 mW He-Ne laser emitting p-polarized light of 632.8 nm wavelength and a 10× objective lens allowed a lateral resolution of ~2 μm. The angle of the incident beam to the interface was fixed to the Brewster angle (53.1°) at 298.2 K. The reflected beam was recorded with a high grade charge-coupled device (CCD) camera (EHDkamPro02, EHD Imaging GmbH, Germany), and the BAM images were digitally saved on the computer hard disk[11, 12, 26].

2.2.4 Fluorescence microscopy (FM)

The film balance system (KSV Minitrough) was mounted onto the stage of an Olympus microscope BX51WI (Tokyo, Japan) equipped with a 100 W mercury lamp (USH-1030L), an objective lens (SLMPlan50×, working distance = 15 mm), and a 3CCD camera with a camera control unit (IK-TU51CU, Toshiba, Japan). A spreading solution of the co-solubilized samples was prepared and doped with 1 mol% of the fluorescence probe (NBD-PC). The image processing and analysis were carried out using an Adobe Photoshop Elements ver. 7.0 (Adobe Systems Inc., CA) software. The total amount of ordered domains (dark contrast regions) was evaluated and expressed as a percentage per frame by dividing the respective frame into dark and bright regions. The resolution was 0.1% and the maximum SD was 8.9%. More details on the FM measurements have been provided in a previous paper[11, 27].

2.2.5 Atomic force microscopy (AFM)

The Langmuir-Blodgett (LB) films were prepared using the KSV Minitrough. Freshly cleaved mica (Okenshoji Co., Tokyo, Japan) was used as the supporting solid substrate for the film deposition (vertical dipping method). At selected surface pressures, a transfer velocity of 5 mm min^{-1} was used for single-layer deposition. The film-forming materials were spread on a 0.15 M NaCl solution at 298.2 K. The transfer occurs in a manner so that the hydrophilic part of the monolayer is in contact with mica while the hydrophobic part is exposed to air. The LB films with a deposition

rate of ~1 were used in the experiments. The AFM images were obtained using an SPA 400 instrument (Seiko Instruments Co., Chiba, Japan) in the tapping mode. The AFM observations were performed in the air at room temperature and provided both topographical and phase contrast images. Other details about the AFM measurements have been reported previously[10, 22].

3 RESULTS AND DISCUSSION

3.1 π–A and ΔV–A isotherms

The surface pressure (π)–molecular area (A) and surface potential (ΔV)–A isotherms for the two-component monolayer of DPPC and *F*8*H*9OH on a 0.15 M NaCl solution at 298.2 K are shown in Fig. 1. The subphase conditions were selected to mimic a biological situation. The DPPC monolayers (*curve 1*) are in a gaseous phase at $A >$ ~1.0 nm^2, where the π and ΔV values are nearly zero. After further compression, DPPC undergoes a first order transition from a liquid-expanded (LE) to a liquid-condensed (LC) phase at π^{eq} = ~11 mN m^{-1} (dashed arrows). Next, the monolayer collapses at π^c = ~55 mN m^{-1} as A decreases. With such phase variations, the ΔV value shows a positive change with decreasing A, i.e., the improvement of monolayer orientations[15, 22, 28, 29]. On the other hand, *F*8*H*9OH (*curve 7*) forms a typical ordered monolayer under the present conditions. The insolubility and monolayer stability of *F*8*H*9OH with respect to the water subphase have been confirmed in a previous paper[21]. The π^c value and limiting area of *F*8*H*9OH monolayers are ~55 mN m^{-1} (at 0.23 nm^2) and ~0.34 nm^2, which represents the cross-sectional area per fluorocarbon chain (~0.30 nm^2)[4]. The *F*8*H*9OH monolayers indicate a negative ΔV value over the entire A. The negative ΔV value for the monolayer made of fluorinated amphiphiles has been well discussed[9, 11, 12]. Thus, the orientation of *F*8*H*9OH monolayers was also improved.

The π–A isotherms for the binary DPPC/*F*8*H*9OH monolayer regularly shift within those for pure components (*curves 1 and 7*). Apparently, the π^{eq} value decreases with increasing mole fraction of *F*8*H*9OH (X_{F8H9OH}), i.e., the solidification of DPPC monolayers was induced by the addition of *F*8*H*9OH[9, 11]. Moreover, the isotherms exhibit a change in π^c against X_{F8H9OH}. The ΔV–A isotherms shift from positive to negative values as X_{F8H9OH} increases[9, 12, 23]. These isotherms provide thermodynamic evidence of the monolayer miscibility between the two components.

3.2 Excess Gibbs free energy

A lateral interaction between DPPC and *F*8*H*9OH monolayers can be analyzed in terms of the excess Gibbs free energy of mixing (ΔG_{mix}^{exc}), which is estimated from the π-A isotherms (Fig. 1). The ΔG_{mix}^{exc} value is calculated from the following equation (Eq 1)[30],

$$\Delta G_{mix}^{exc} = \int_0^{\pi} (A_{12} - X_1 A_1 - X_2 A_2)\, d\pi \quad (1)$$

where A_i and X_i are the molecular area and mole fraction of component i, respectively, and A_{12} is the mean molecular area in the binary monolayer. For identical interactions between the two components, the value of ΔG_{mix}^{exc} is zero, i.e., they are ideally mixed in the monolayer or are completely immiscible similar to a patched packing[31, 32]. A negative value of ΔG_{mix}^{exc} indicates that an attractive interaction exists between the two components. The ΔG_{mix}^{exc} value is plotted as the functions of X_{F8H9OH} and π in Fig. 2. The plots can be divided into two regions at the boundary of X_{F8H9OH} = 0.5. At $0 < X_{F8H9OH} \leq 0.3$, a complicated behavior against surface pressure was observed. This is attributed to the phase transition of monolayers from disordered to ordered states upon compression: e.g., the monolayer for X_{F8H9OH} = 0.1 at 5 mN m^{-1} and at $\pi \geq 15$ mN m^{-1} is in disordered and ordered phases, respectively (see *curve 2* in Fig. 1). The ΔG_{mix}^{exc} value below 25 mN m^{-1} is positive. Considering the variation in π^{eq} with respect to X_{F8H9OH} (Fig. 1), the

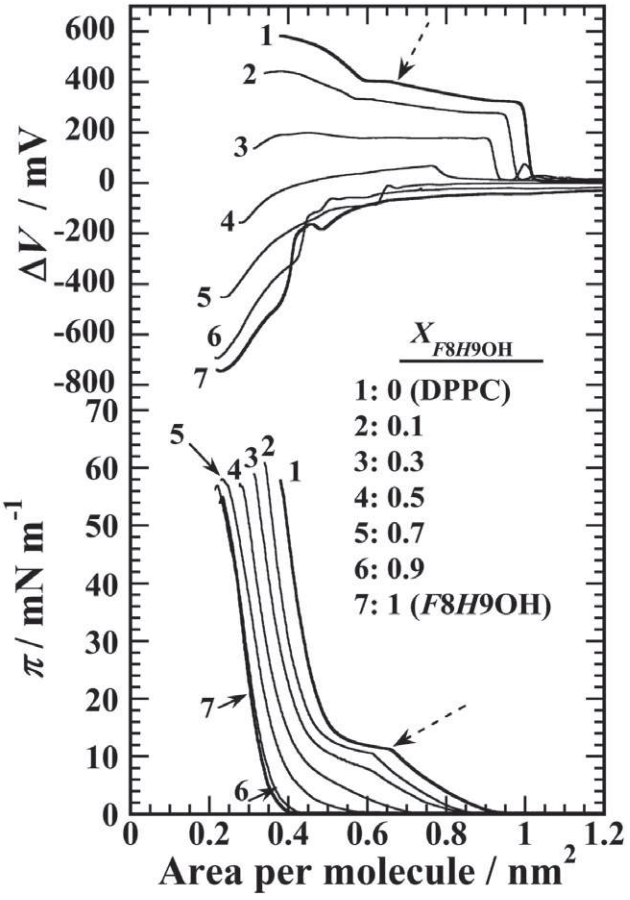

Fig. 1 The π–A and ΔV–A isotherms of the binary DPPC/*F*8*H*9OH monolayers on 0.15 M NaCl at 298.2 K.

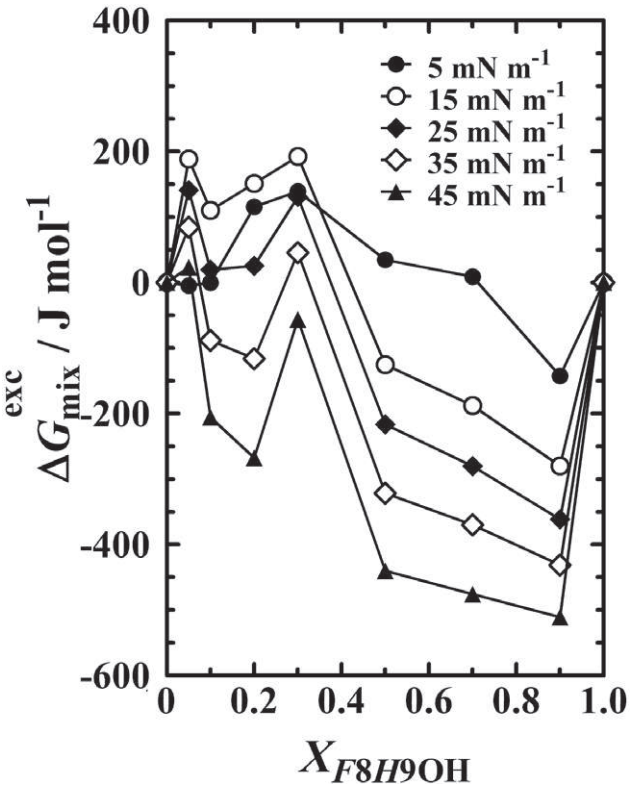

Fig. 2 Excess Gibbs free energy of mixing (ΔG^{exc}_{mix}) of the binary DPPC/*F*8*H*9OH monolayers as a function of X_{F8H9OH} at typical surface pressures on 0.15 M NaCl at 298.2 K.

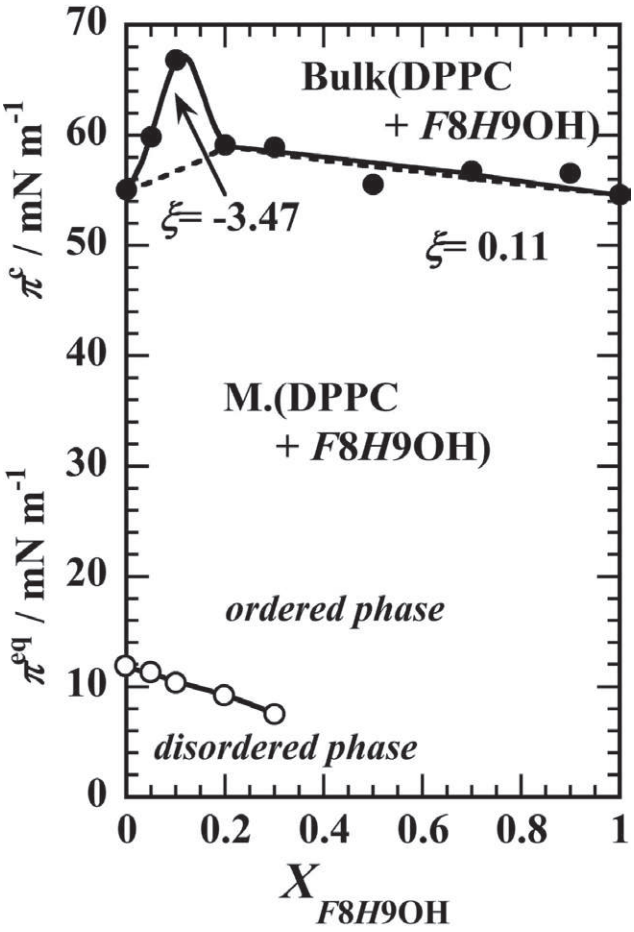

Fig. 3 Two-dimensional phase diagrams based on the variation of the transition pressure (π^{eq}: open circle) and collapse pressure (π^{c}: solid circle) on 0.15 M NaCl at 298.2 K as a function of X_{F8H9OH}. The dashed lines were calculated according to eq 2 for $\xi = 0$. The solid line at high surface pressures was obtained by curve fitting of experimental π^{c} to eq 2. **M**. indicates a mixed monolayer formed by DPPC and *F*8*H*9OH species, whereas **Bulk** denotes a solid phase of DPPC and *F*8*H*9OH (''bulk phase" so called ''solid phase").

change of ΔG^{exc}_{mix} within 200 J mol^{-1} is not significantly important for this analysis. On the other hand, the ΔG^{exc}_{mix} value in $0.5 \le X_{F8H9OH} < 1$ decreases with increasing π. The monolayers are in ordered states over the entire surface pressures above 1 mN m^{-1} (Fig. 1). At a constant π (e.g., 35 mN m^{-1}), the minimum ΔG^{exc}_{mix} value is produced at $X_{F8H9OH} = 0.9$, indicating that the affinity between DPPC and *F*8*H*9OH monolayers becomes the largest at $X_{F8H9OH} = 0.9$.

3.3 Two-dimensional phase diagrams

A phase diagram (π vs. X_{F8H9OH}) for the binary system at 298.2 K is shown in Fig. 3. As mentioned above, the solidification of DPPC monolayers induced by the *F*8*H*9OH addition results from the decrease in π^{eq} against X_{F8H9OH}. Therefore, the slope of $\partial\pi^{eq}/\partial X$ can be considered to express the degree of the solidification (negative) or fluidization (positive)[8, 26]. The inclination for the DPPC/*F*8*H*9OH system ($0 \le X_{F8H9OH} \le 0.3$) is ~ -14 mN m^{-1}. In the case of the binary DPPC/*F*8*H*11OH system, where the π^{eq} value also decreases linearly as $X_{F8H11OH}$ increases ($0 \le X_{F8H11OH} \le 0.2$), the $\partial\pi^{eq}/\partial X$ value is ~ -33 mN m^{-1} [11], i.e., the magnitude of the solidification for the *F*8*H*11OH system is more than twice larger compared to that for the *F*8*H*9OH system. On the other hand, the two-component systems of DPPC and homologous shorter alcohols such as *F*8*H*5OH and *F*8*H*7OH respectively indicate positive and negative but nonlinear variations in π^{eq} with respect to X_{F8HmOH}[12, 20].

The experimental π^{c} values also vary against X_{F8H9OH}. Therefore, the two components may be miscible within a monolayer state. The coexistence of a phase boundary between the monolayer phase (2D) and bulk phase (3D) of the molecules that are spread on the surface can be theoretically simulated by using the Joos equation under the assumption of a regular surface mixture[33, 34],

$$1 = x_1^s \exp\{(\pi_m^c - \pi_1^c)\omega_1 / kT \exp\{\xi (x_2^s)^2\} + x_2^s \{\exp(\pi_m^c - \pi_2^c)\omega_2 / kT\} \exp\{\xi (x_1^s)^2\} \quad (2)$$

where x_1^s and x_2^s denote the respective mole fractions in the two-component monolayer consisting of components 1 and 2; π_1^c and π_2^c are the respective collapse pressures of components 1 and 2 and π_m^c is the collapse pressure of the binary monolayer at a given composition of x_1^s (or x_2^s); ω_1 and ω_2 are the corresponding molecular areas at monolayer collapse pressure; ξ is the interaction parameter; and kT is the product of Boltzmann constant and Kelvin temperature. The solid curve at higher surface pressures could be obtained by adjusting the interaction parameter in Eq 2, to achieve the best fit for the experimental π^c values. Therefore, two different interaction parameters are obtained: $\xi = -3.47$ for $0 \le X_{F8H9OH} \le 0.2$ and $\xi = 0.11$ for $0.2 \le X_{F8H9OH} \le 1$. In the latter region, the two components are regarded as almost ideal mixing. The interaction energy ($\Delta\varepsilon$) is given as follows:

$$\Delta\varepsilon = \xi RT/z, \quad (3)$$

where z is the number of nearest neighbors per molecule, equal to six, in a close-packed monolayer and the interaction energy is $\Delta\varepsilon = \varepsilon_{12} - (\varepsilon_{11} + \varepsilon_{22})/2$[33]; ε_{12} denotes the potential interaction energy between components 1 and 2. The calculated ξ and $\Delta\varepsilon$ are listed in Table 1, where the values for the other binary systems of DPPC/*F*8*H*mOH are also listed for comparison purpose[11, 12, 20]. The ξ value for all the systems except for $m = 5$ is quite larger in magnitude in the small X_{F8HmOH} region. In contrast, in the large X_{F8HmOH} region, the two components cause almost the ideal interaction. Therefore, the mode of mutual interactions is different at the boundary between $m = 5$ and 7. Moreover, the variation in π^{eq} with X_{F8HmOH} supports the boundary; convex variations (fluidization) for $m = 5$ and linear or nonlinear negative values (solidification) for $m \ge 7$. Among the systems for $m \ge 7$, *F*8*H*11OH indicates the largest solidifying effect on DPPC monolayers. The extension of methylene (–CH_2–) in a partially fluorinated chain significantly contributes to the solidifying effect. However, the degree of the effect is not reflected in the ξ value. This may be due to the fact that the monolayer is in the closest packing at π^c. Thus, it is suggested that the mode of the binary interaction at low surface pressures is different from that at high surface pressures. Indeed, such opposite mode of interactions was remarkably observed for the DPPC/*F*8*H*7OH system[20].

Table 1 Interaction Parameters and Energies for the DPPC/*F*8*Hm*OH systems on 0.15 M NaCl.

m	T / K	X_{F8HmOH}	ξ	$\Delta\varepsilon$/J mol^{-1}
5*	293.2	$0 \le X_{F8H5OH} \le 1$	1.15	470
7§	298.2	$0 \le X_{F8H7OH} \le 0.3$	−3.03	−1267
		$0.3 \le X_{F8H7OH} \le 1$	0.67	277
9	298.2	$0 \le X_{F8H9OH} \le 0.2$	−3.47	−1434
		$0.2 \le X_{F8H9OH} \le 1$	0.11	45
11†	298.2	$0 \le X_{F8H11OH} \le 0.3$	−3.13	−1293
		$0.3 \le X_{F8H11OH} \le 1$	−0.04	−17

* ref. [12]
§ ref. [20]
† ref. [11]

3.4 BAM observations

The phase behavior of the binary monolayer has been observed directly on a 0.15 M NaCl solution by BAM. The representative images are shown in Fig. 4. In the BAM observation, the dark and bright contrasts are respectively assigned to LE (or disordered) and LC (or ordered) phases of monolayers. All the BAM images below π^{eq} are optically homogeneous (data not shown). As for DPPC monolayers (*the first column*), LC domains begin to be formed at $\pi^{eq} = \sim 11$ mN m^{-1}, and then they grow in size and number with increasing surface pressures. The detailed analysis on the morphology of DPPC monolayers has already been reported elsewhere[11, 27]. On the other hand, *F*8*H*9OH monolayers exhibit optically homogeneous images over the entire π as easily expected from the π–*A* isotherm (*curve 7* in Fig. 1). The BAM images for the binary monolayer shown here indicate different morphologies from those for DPPC alone. A small amount addition of *F*8*H*9OH ($X_{F8H9OH} = 0.05$) induces a size increment of the ordered domains, where the domain shape does not change significantly. With further addition ($X_{F8H9OH} = 0.1$), the magnitude of the domain growth becomes larger and the domain shape also varies to become round. In complete contrast to the size increase, a high dispersion of the ordered domains is caused at $X_{F8H9OH} = 0.2$. This phenomenon is often observed for a system containing fluorinated amphiphiles[10, 11]. Above $X_{F8H9OH} = 0.2$, the BAM images are homogeneously dark over the entire π (data not shown), i.e., a fine dispersion of the two components is induced within the BAM resolution.

3.5 FM observations

The *in situ* micrographs for the DPPC/*F*8*H*9OH monolayer were obtained with fluorescence microscopy (FM). In contrast to BAM, FM is an indirect technique for the visualization of monolayers at the surface because of the use of a fluorescent probe (in this case NBD-PC). In the FM observation, however, the phase behavior can be caught with higher resolution and magnification. The bright and dark contrasts correspond to the disordered and ordered phases, respectively, as opposed to the corresponding BAM image (Fig. 4). In fact, the FM image of DPPC monolayers (*the first column*) is clearer in contrast compared to the BAM image. The shape of the LC domain is characteristic

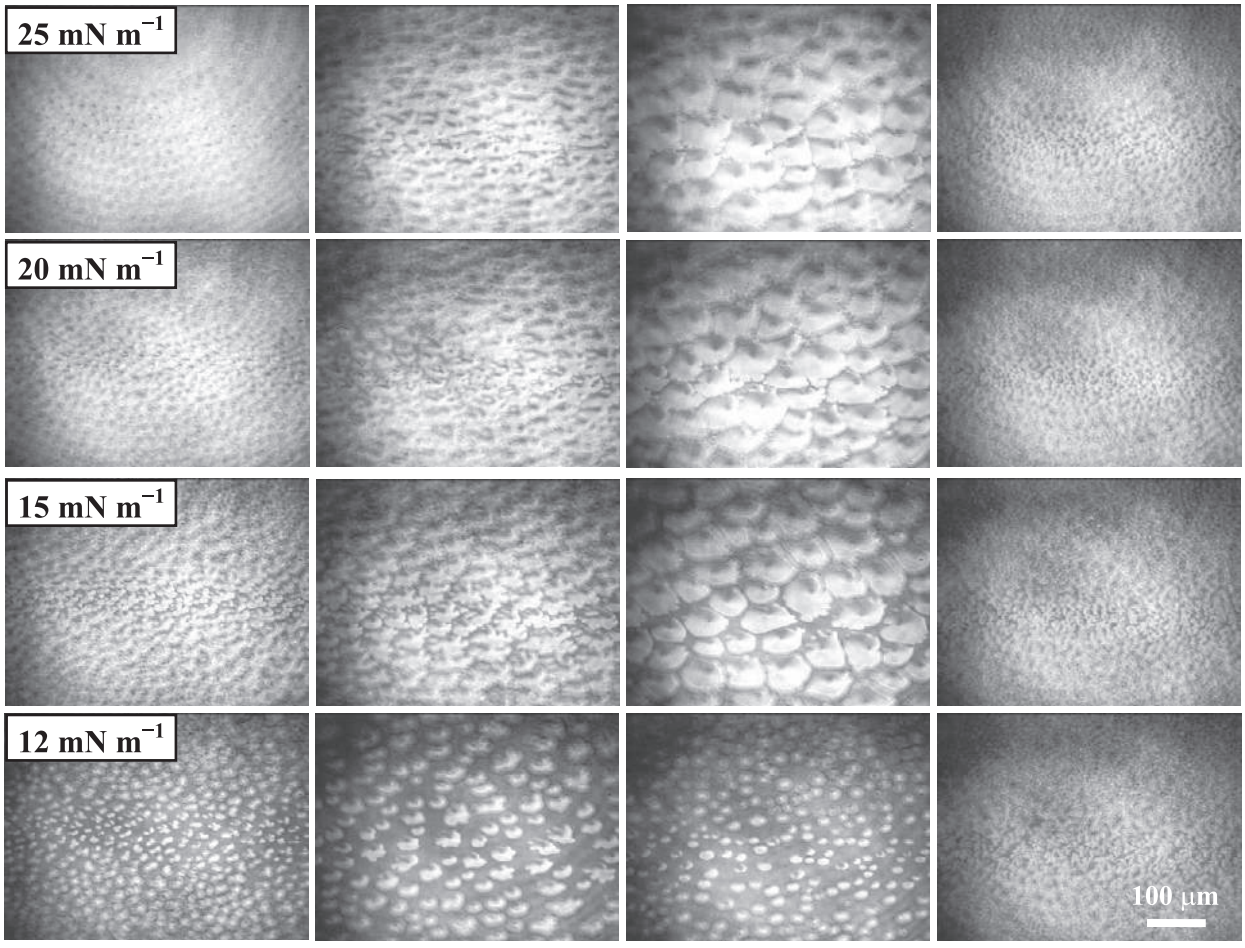

Fig. 4 BAM images of the binary DPPC/*F*8*H*9OH monolayers for X_{F8H9OH} = 0 (DPPC), 0.05, 0.1, and 0.2 at 12, 15, 20, and 25 mN m^{-1} on 0.15 M NaCl at 298.2 K. The scale bar in the lower right represents 100 μm.

of DPPC monolayers, which has been discussed well[11, 12, 35, 36]. At $X_{F8H9OH} = 0.05$, three anticlockwise arms of the LC domain (DPPC) change to a round form, which closes the disordered domain at its center. Moreover, these domains grow in size upon compression and accordingly the ratio of ordered domains per frame increases. Similar morphology is observed even at $X_{F8H9OH} = 0.1$. However, the disordered domain (bright) located at the center of ordered domain disappears. It is widely accepted that a domain formation is controlled by the balance of line tension at the boundary between the disordered and ordered domains and long-range dipole-dipole interactions between the ordered domains[37]. Therefore, these shape variations mean that the line tension rather than the dipole interaction significantly contributes to the domain formation. On the other hand, the FM images at $X_{F8H9OH} = 0.2$ show a different behavior from those at $X_{F8H9OH} = 0.05$ and 0.1. The domain shape takes on the characteristic form of DPPC monolayers once more. This phenomenon suggests that the large amount addition of *F*8*H*9OH has few effects on the line tension or the dipole interaction with regard to the domain formation. Therefore, the mode of interaction between the two components is found to change significantly at $X_{F8H9OH} = 0.2$, which is in good agreement with the result of phase diagram at high surface pressures (Fig. 3). In $X_{F8H9OH} \geq 0.3$, the FM images remain optically homogeneous in contrast regardless of surface pressure. Unfortunately, this is attributed to the resolution limit of FM apparatus similar to the BAM observation. Therefore, the morphological analyses in $X_{F8H9OH} \geq 0.3$ were carried out in the next section. Figure 6 shows the plots of a percentage of the ordered domain per frame of FM images (Fig. 5), as a function of π. The ordered domain ratio for the entire compositions here increases monotonically with increasing π and finally reaches ~90% at 30 mN m^{-1}, which is the same behavior as the *F*8*H*7OH and *F*8*H*11OH systems[11, 20]. Therefore, this result supports the evidence of no fluidizing effect of *F*8*H*9OH on DPPC monolayers. To understand the distribution of each

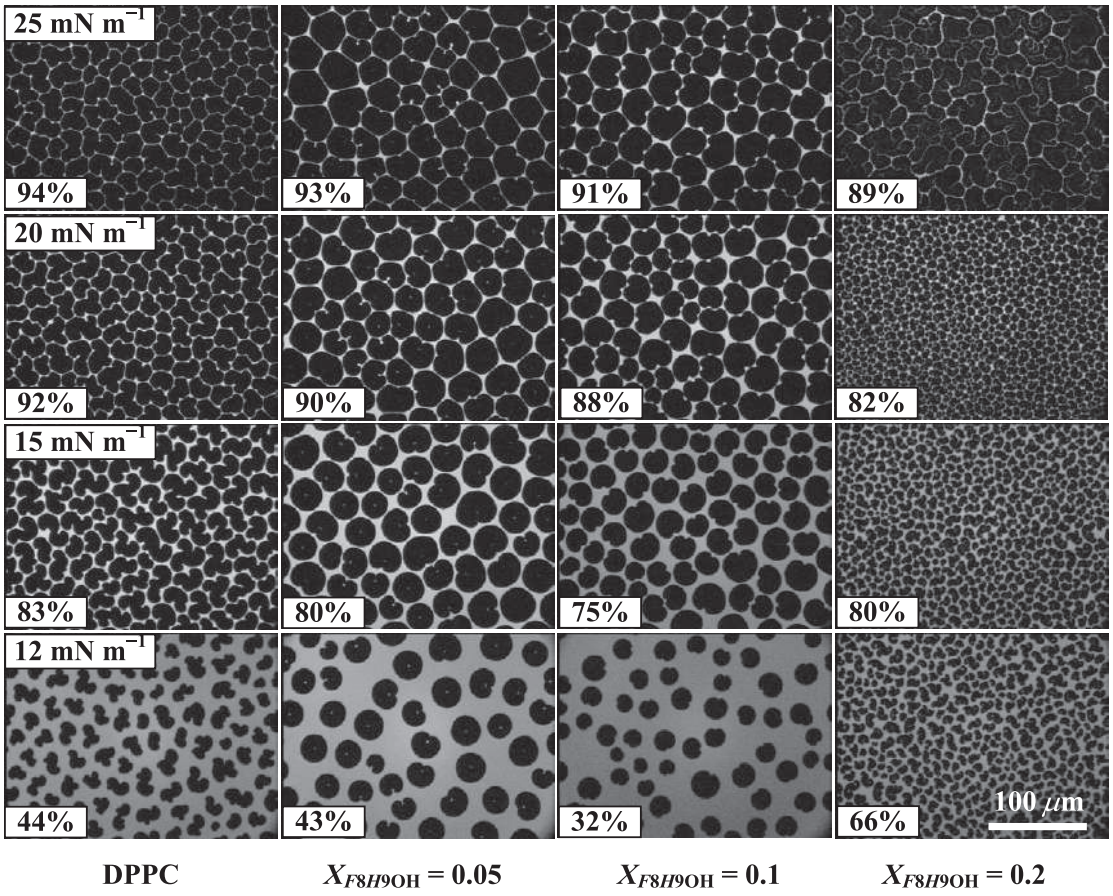

Fig. 5 FM images of the binary DPPC/*F*8*H*9OH monolayers for X_{F8H9OH} = 0 (DPPC), 0.05, 0.1, and 0.2 at 12, 15, 20, and 25 mN m^{-1} on 0.15 M NaCl at 298.2 K. The monolayers contain 1 mol% of fluorescent probe (NBD-PC). The percentage (%) in lower-left corner exhibits the ratio of ordered domains (dark contrast) per micrograph. The scale bar in the lower right represents 100 μm.

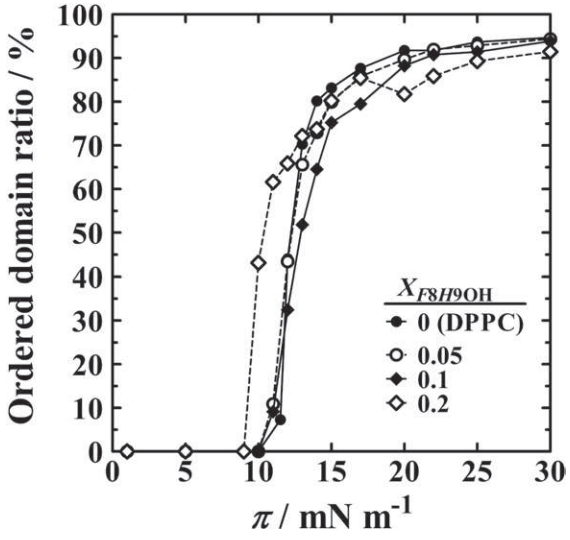

Fig. 6 Surface-pressure dependence of the ratio of ordered domain area (dark contrast) in FM images of the binary DPPC/*F*8*H*9OH monolayers for X_{F8H9OH} = 0, 0.05, 0.1, and 0.2.

component in FM images, the following property needs to be taken into consideration as well; *F*8*H*9OH forms an ordered monolayer (dark contrast) in the temperature range from 283.2 to 303.2[21], whereas DPPC domains are expressed by both bright (LE) and dark (LC) contrasts depending on surface pressure. If the *F*8*H*9OH domain is indicated by bright contrast (disordered), the ordered domain ratio should decrease quantitatively with an increase in X_{F8H9OH}. In this case, the ratio is kept to high values in spite of the X_{F8H9OH} increment. Thus, the ordered domain in the binary system is composed of both DPPC and *F*8*H*9OH. On the other hand, the disordered region corresponds to the LE phase of DPPC monolayers. These distributions are also supported by the domain variation as mentioned above.

3.6 AFM observation

One-layer Langmuir-Blodgett (LB) films transferred onto a mica for the DPPC/*F*8*H*9OH system have been visualized by AFM. The AFM topography for pure DPPC monolayers at 35 mN m^{-1} is optically homogeneous (data not shown).

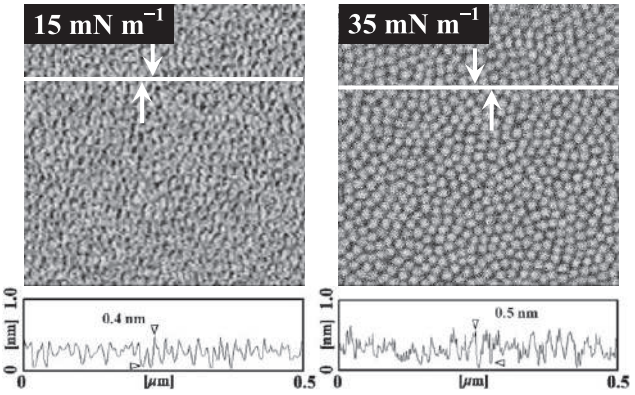

Fig. 7 Typical AFM topographic images of single *F*8*H*9OH monolayers at 15 and 35 mN m^{-1}. The scan area is 500 × 500 nm. The cross-sectional profiles along the scanning line (white line) are given just below the respective AFM images. The height difference between the arrows is indicated in the cross-sectional profile.

The AFM images for single *F*8*H*9OH monolayers at 15 and 35 mN m^{-1} are shown in Fig. 7. The image at 15 mN m^{-1} indicates a rough pattern with the height difference of <0.4 nm from the surroundings (see the cross section) although *F*8*H*9OH forms ordered films. With a further increase to π = 35 mN m^{-1}, the morphology shows distinct and round-shaped assemblies. The organization shows a monodispersed 2D surface micelles with a characteristic diameter of 19.1 ± 3.8 nm and height of 0.4 ± 0.1 nm. The surface micelle is roughly estimated to be composed of ~840 molecules. The size of surface micelles made of partially fluorinated carboxylic acids has been reported to be >17 nm in diameter[17]. A partially fluorinated alkane forms the surface micelle with a diameter of 30 nm[38]. Thus, the range of a few tens of nanometer in diameter is considered to be characteristic at the surface micelle of partially fluorinated amphiphiles. The micelle formation and appearance are quite similar to the homolog of *F*8*H*7OH[20]. In that case, however, the surface micelle gathers at 35 mN m^{-1} so that the image becomes hardly visible. Kato and co-workers have reported that the surface micelle composed of partially fluorinated long-chain acids is very stable and does not fuse to each other even at high surface pressures[17]. Thus, the *F*8*H*9OH micelle shows opposite behavior than *F*8*H*7OH. The formation of surface micelles is often observed in the LB film for partially fluorinated compounds[17, 18, 38]. Therefore, the key factors to form the 2D micelle are considered to be a weak van der Waals interaction between the fluorocarbons[20] and a further reclining fluorocarbon moieties at the linkage (CF_2–CH_2). Considering the fact that no micelle is formed for *F*8*H*5OH and *F*8*H*11OH[11, 12], this result suggests that the stability of surface micelles strongly depends on the total hydrophobic chain length and/or the degree of fluorination in hydrophobic chains.

Figure 8 shows the AFM images for the two-component system at X_{F8H9OH} = 0.3, 0.5, and 0.7, where indistinguishable morphological changes are observed in the *in situ* BAM and FM measurements. The AFM image at X_{F8H9OH} = 0.3 at 15 mN m^{-1} exhibits lots of dark "cracks," i.e., narrow regions with lower thickness. The fact that the occupied area of cracks in the image is smaller than the surrounding bright regions, the lower cracks probably consist mainly of *F*8*H*9OH. The depth of the cracks (~0.7 nm) suggests that the hydrophobic chains of *F*8*H*9OH are less oriented. Similar morphology indicating the cracks is observed for the binary DPPC/*F*8*H*11OH system[11]. Thus, the poor orientation is considered to be strongly affected by the further reclining perfluorooctyl moieties at the linkage (CF_2–CH_2) in *F*8*H*9OH. As π increases to 35 mN m^{-1}, the cracks decrease in occupied area and their depth also reduces to ~0.4 nm. The former supports the miscibility of the two components at the nanometer scale. Furthermore, the improved orientation of hydrocarbon chains in *F*8*H*9OH is confirmed by the decrease in crack depth. On the other hand, above X_{F8H9OH} = 0.5, the AFM topographies indicate entirely different morphologies. At X_{F8H9OH} = 0.5, the DPPC monolayer forms a wormlike (bright contrast) domain separated by a sea of *F*8*H*9OH molecules at 15 mN m^{-1}. The π increase changes the appearance to roughly circular islands with a diameter of ~45 nm (35 mN m^{-1}). This behavior suggests that the phase separation at the nanometer scale is promoted by the composition. The similar but unclear-contrast topographies are exhibited at X_{F8H9OH} = 0.7. In a strict sense, the DPPC-rich domains (bright contrast) are dispersed to many noncircular fragments by the surrounding *F*8*H*9OH molecules. It is worthwhile that surface micelles are formed at X_{F8H9OH} = 0.9 at 15 mN m^{-1}. Compared to the surface micelles in Fig. 7, the contrast is somewhat unclear due to the miscibility between the two components and/or the decrease in *F*8*H*9OH purity. The binary DPPC/*F*8*H*7OH system at X_{F8H7OH} = 0.9 exhibits no micelles in the AFM image[20], i.e., these images reveal that the surface micelle made of *F*8*H*9OH is more stable. At 35 mN m^{-1}, however, the surface micelle disappears and the morphology becomes flat within the height difference of <0.2 nm. This is attributed to the enhancement of miscibility between the two components upon compression[20].

4 CONCLUSION

In this study, it was found that *F*8*H*9OH is miscible with DPPC in binary monolayer state. The π–*A* and ΔV–*A* isotherms were measured as a function of X_{F8H9OH}. The isotherm data was used to evaluate the excess Gibbs free energy of mixing and phase diagram of surface pressure vs.

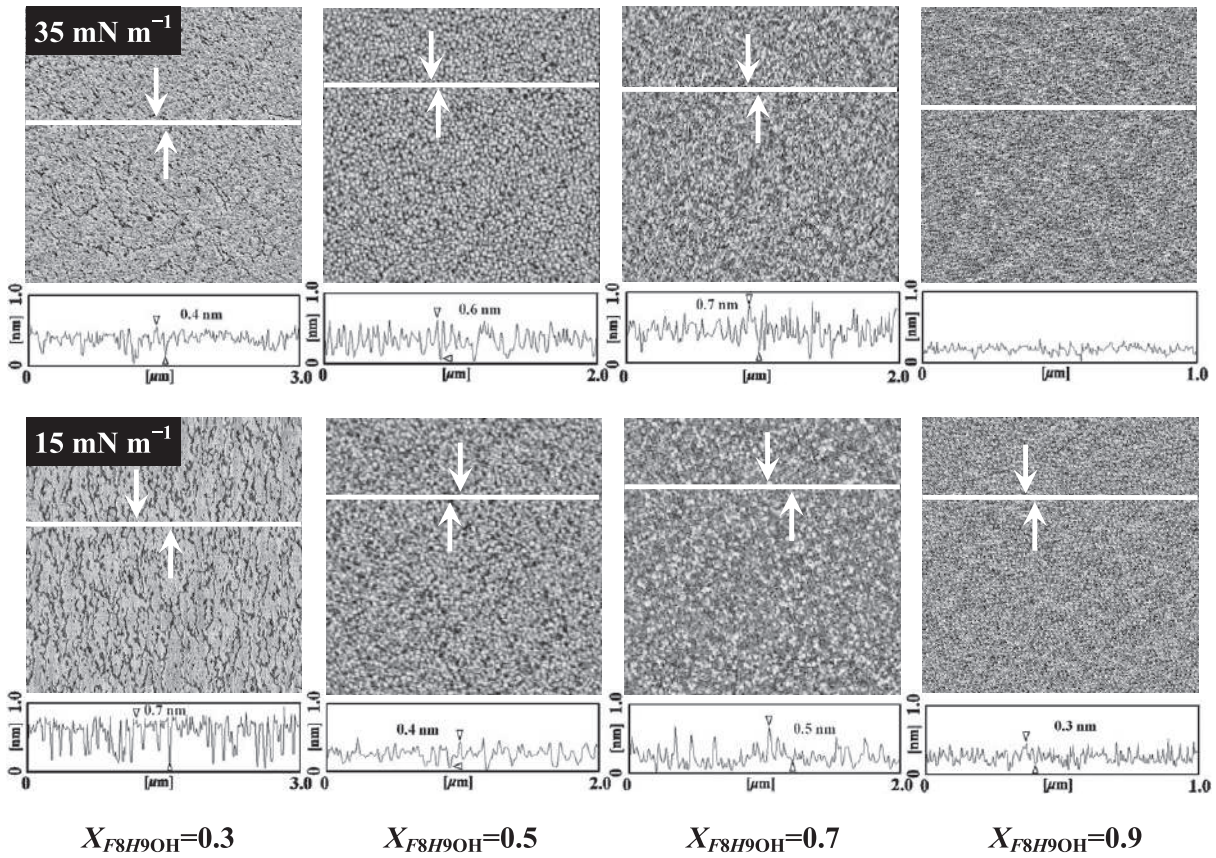

Fig. 8 Typical AFM topographic images of the binary DPPC/*F*8*H*9OH monolayers for X_{F8H9OH} = 0.3, 0.5, and 0.7 at 15 and 35 mN m^{-1}. The cross-sectional profiles along the scanning line (white line) are given just below the respective AFM images. The height difference between the arrows is indicated in the cross-sectional profile.

X_{F8H9OH}. These analyses provided thermodynamic evidence of the binary miscibility. Although *F*8*Hm*OH (m = 5, 7, 9, and 11) is miscible with DPPC monolayers, the interactions are different: a fluidizing effect on DPPC for m = 5 and a solidifying effect for m = 7, 9, and 11 were observed. Moreover, the *in situ* morphological observations by BAM and FM also supported the miscibility on the micrometer scale. The AFM topography of the one-layer LB film shows the formation of a monodispersed 2D surface micelle of *F*8*H*9OH, and the micelle was found to be more stable than that made by *F*8*H*7OH. The AFM images showed the dispersion of DPPC monolayers in nanometer scale induced by the addition of *F*8*H*9OH. This study also described the importance of CF_2–CH_2 linkages in fluorinated amphiphiles for understanding their physicochemical properties and interactions with other compounds.

ACKNOWLEDGEMENTS

This work was supported by a Grant-in-Aid for Scientific Research 23510134 from the Japan Society for the Promotion of Science (JSPS). It was also supported by a Grant-in-Aid for Young Scientists (B) 25790020 from JSPS (H.N.).

REFERENCES

1) Veldhuizen, R.; Nag, K.; Orgeig, S.; Possmayer, F. The role of lipids in pulmonary surfactant. *Biochim. Biophys. Acta* **1408**, 90-108 (1998).
2) Krüger, P.; Baatz, J. E.; Dluhy, R. A.; Lösche, M. Effect of hydrophobic surfactant protein SP-C on binary phospholipid monolayers. Molecular machinery at the air/water interface. *Biophys. Chem.* **99**, 209-228 (2002).
3) Yu, S.-H.; Possmayer, F. Lipid compositional analysis of pulmonary surfactant monolayers and monolayer-associated reservoirs. *J. Lipid Res.* **44**, 621-629 (2003).
4) Riess, J. G. Fluorous micro- and nanophases with a biomedical perspective. *Tetrahedron* **58**, 4113-4131 (2002).
5) Kissa, E., *Fluorinated Surfactants and Repellents. 2nd ed., revised and expanded*. Surfactant Science Series 97; Hubbard, A. T., Ed.; Marcel Dekker Inc.: Basel, New York, pp 1-615 (2001).

6) Riess, J. G. Oxygen carriers("blood substitutes")–raison d'etre, chemistry, and some physiology. *Chem. Rev.* **101**, 2797-2920(2001).
7) Krafft, M. P.; Riess, J. G. Chemistry, physical chemistry, and uses of molecular fluorocarbon-hydrocarbon diblocks, triblocks, and related compounds–unique "apolar" components for self-assembled colloid and interface engineering. *Chem. Rev.* **109**, 1714-1792 (2009).
8) Nakahara, H.; Shibata, O. Langmuir monolayer miscibility of perfluorocarboxylic acids with biomembrane constituents at the air-water interface. *J. Oleo Sci.* **61**, 197-210(2012).
9) Nakahara, H.; Nakamura, S.; Kawasaki, H.; Shibata, O. Properties of two-component Langmuir monolayer of single chain perfluorinated carboxylic acids with dipalmitoylphosphatidylcholine(DPPC). *Colloids Surf. B* **41**, 285-298(2005).
10) Nakahara, H.; Ohmine, A.; Kai, S.; Shibata, O. Monolayer compression induces fluidization in binary system of partially fluorinated alcohol(*F*4*H*11OH)with DPPC. *J. Oleo Sci.*, **62**, 271-281(2013).
11) Nakahara, H.; Krafft, M. P.; Shibata, A.; Shibata, O. Interaction of a partially fluorinated alcohol(*F*8*H*11OH) with biomembrane constituents in two-component monolayers. *Soft Matter* **7**, 7325-7333(2011).
12) Nakamura, S.; Nakahara, H.; Krafft, M. P.; Shibata, O. Two-component Langmuir monolayers of single-chain partially fluorinated amphiphiles with dipalmitoylphosphatidylcholine(DPPC). *Langmuir* **23**, 12634-12644 (2007).
13) Lehmler, H.-J.; Bummer, P. M. Behavior of 10-(perfluorohexyl)-decanol, a partially fluorinated analog of hexadecanol, at the air-water interface. *J. Fluorine Chem.* **117**, 17-22(2002).
14) Lehmler, H.-J.; Bummer, P. M. Mixing behavior of 10-(perfluorohexyl)-decanol and DPPC. *Colloids Surf. B* **44**, 74-81(2005).
15) Hiranita, T.; Nakamura, S.; Kawachi, M.; Courrier, H. M.; Vandamme, T. F.; Krafft, M. P.; Shibata, O. Miscibility behavior of dipalmitoylphosphatidylcholine with a single-chain partially fluorinated amphiphile in Langmuir monolayers. *J. Colloid Interf. Sci.* **265**, 83-92(2003).
16) Lehmler, H.-J.; Jay, M.; Bummer, P. M. Mixing of Partially Fluorinated Carboxylic Acids and Their Hydrocarbon Analogues with Dipalmitoylphosphatidylcholine at the Air-Water Interface. *Langmuir* **16**, 10161-10166(2000).
17) Kato, T.; Kameyama, M.; Ehara, M.; Iimura, K.-i. Monodisperse Two-Dimensional Nanometer Size Clusters of Partially Fluorinated Long-Chain Acids. *Langmuir* **14**, 1786-1798(1998).
18) Ren, Y.; Iimura, K.; Kato, T. Surface micelles of $F(CF_2)_m(CH_2)_{22}COOH$ on the aqueous cadmium acetate solution investigated in situ and ex situ by infrared spectroscopy. *J. Phys. Chem. B* **106**, 1327-1333(2002).
19) Arora, M.; Bummer, P. M.; Lehmler, H.-J. Interaction of a partially fluorinated heptadecanoic acid with diacyl phosphatidylcholines of varying chain length. *Langmuir* **19**, 8843-8851(2003).
20) Nakahara, H.; Hirano, C.; Fujita, I.; Shibata, O. Interfacial properties in Langmuir monolayers and LB films of DPPC with partially fluorinated alcohol(*F*8*H*7OH). *J. Oleo Sci.*, **62**, 1017-1027(2013).
21) Nakahara, H.; Nakamura, S.; Okahashi, Y.; Kitaguchi, D.; Kawabata, N.; Sakamoto, S.; Shibata, O. Examination of fluorination effect on physical properties of saturated long-chain alcohols by DSC and Langmuir monolayer. *Colloids Surf. B* **102**, 472-478(2013).
22) Nakahara, H.; Lee, S.; Sugihara, G.; Shibata, O. Mode of interaction of hydrophobic amphiphilic α-helical peptide/dipalmitoylphosphatidylcholine with phosphatidylglycerol or palmitic acid at the air-water interface. *Langmuir* **22**, 5792-5803(2006).
23) Nakahara, H.; Tsuji, M.; Sato, Y.; Krafft, M. P.; Shibata, O. Langmuir monolayer miscibility of single-chain partially fluorinated amphiphiles with tetradecanoic acid. *J. Colloid Interf. Sci.* **337**, 201-210(2009).
24) Nakahara, H.; Shibata, O.; Moroi, Y. Examination of surface adsorption of sodium chloride and sodium dodecyl sulfate by surface potential measurement at the air/solution interface. *Langmuir* **21**, 9020-9022 (2005).
25) Nakahara, H.; Shibata, O.; Rusdi, M.; Moroi, Y. Examination of Surface Adsorption of Soluble Surfactants by Surface Potential Measurement at the Air/Solution Interface. *J. Phys. Chem. C* **112**, 6398-6403(2008).
26) Matsumoto, Y.; Nakahara, H.; Moroi, Y.; Shibata, O. Langmuir monolayer properties of perfluorinated double long-chain salts with divalent counterions of separate electric charge at the air-water interface. *Langmuir* **23**, 9629-9640(2007).
27) Nakahara, H.; Lee, S.; Krafft, M. P.; Shibata, O. Fluorocarbon-hybrid pulmonary surfactants for replacement therapy - a Langmuir monolayer study. *Langmuir* **26**, 18256-18265(2010).
28) Nakahara, H.; Lee, S.; Shibata, O. Pulmonary surfactant model systems catch the specific interaction of an amphiphilic peptide with anionic phospholipid. *Biophys. J.* **96**, 1415-1429(2009).
29) Hoda, K.; Nakahara, H.; Nakamura, S.; Nagadome, S.; Sugihara, G.; Yoshino, N.; Shibata, O. Langmuir monolayer properties of the fluorinated-hydrogenated hybrid amphiphiles with dipalmitoylphosphatidylcholine (DPPC). *Colloids Surf. B* **47**, 165-175(2006).
30) Goodrich, F. C. In *Proceeding of 2nd International Congress on Surface Activity, J. H. Schulman ed.*, London, 1957; Butterworth & Co.: London, 1957; p 85.

31) Marsden, J.; Schulman, J. H. *Trans. Faraday Soc.* **34**, 748-758(1938).
32) Shah, D. O.; Schulman, J. H. *J. Lipid Res.* **8**, 215-226 (1967).
33) Joos, P.; Demel, R. A. The interaction energies of cholesterol and lecithin in spread mixed monolayers at the air-water interface. *Biochim. Biophys. Acta* **183**, 447-457(1969).
34) Savva, M.; Acheampong, S. The interaction energies of cholesterol and 1,2-dioleoyl-sn-glycero-3-phosphoethanolamine in spread mixed monolayers at the air-water interface. *J. Phys. Chem. B* **113**, 9811-9820 (2009).
35) Leiske, D. L.; Meckes, B.; Miller, C. E.; Wu, C.; Walker, T. W.; Lin, B.; Meron, M.; Ketelson, H. A.; Toney, M. F.; Fuller, G. G. Insertion mechanism of a poly(ethylene oxide)-poly(butylene oxide)block copolymer into a DPPC monolayer. *Langmuir* **27**, 11444-11450(2011).
36) Scholtysek, P.; Li, Z.; Kressler, J.; Blume, A. Interactions of DPPC with semitelechelic poly(glycerol methacrylate)s with perfluoroalkyl end groups. *Langmuir* **28**, 15651-15662(2012).
37) Thirumoorthy, K.; Nandi, N.; Vollhardt, D. Role of dipolar interaction in the mesoscopic domains of phospholipid monolayers: dipalmitoylphosphatidylcholine and dipalmitoylphosphatidylethanolamine. *Langmuir* **23**, 6991-6996(2007).
38) Maaloum, M.; Muller, P.; Krafft, M. P. Lateral and Vertical Nanophase Separation in Langmuir-Blodgett Films of Phospholipids and Semifluorinated Alkanes. *Langmuir* **20**, 2261-2264(2004).